



## Experiment Report Form

**The double page inside this form is to be filled in by all users or groups of users who have had access to beam time for measurements at the ESRF.**

Once completed, the report should be submitted electronically to the User Office via the User Portal:

<https://www.esrf.fr/misapps/SMISWebClient/protected/welcome.do>

### ***Reports supporting requests for additional beam time***

Reports can be submitted independently of new proposals – it is necessary simply to indicate the number of the report(s) supporting a new proposal on the proposal form.

The Review Committees reserve the right to reject new proposals from groups who have not reported on the use of beam time allocated previously.

### ***Reports on experiments relating to long term projects***

Proposers awarded beam time for a long term project are required to submit an interim report at the end of each year, irrespective of the number of shifts of beam time they have used.

### ***Published papers***

All users must give proper credit to ESRF staff members and proper mention to ESRF facilities which were essential for the results described in any ensuing publication. Further, they are obliged to send to the Joint ESRF/ ILL library the complete reference and the abstract of all papers appearing in print, and resulting from the use of the ESRF.

Should you wish to make more general comments on the experiment, please note them on the User Evaluation Form, and send both the Report and the Evaluation Form to the User Office.

### **Deadlines for submission of Experimental Reports**

- 1st March for experiments carried out up until June of the previous year;
- 1st September for experiments carried out up until January of the same year.

### **Instructions for preparing your Report**

- fill in a separate form for each project or series of measurements.
- type your report, in English.
- include the reference number of the proposal to which the report refers.
- make sure that the text, tables and figures fit into the space available.
- if your work is published or is in press, you may prefer to paste in the abstract, and add full reference details. If the abstract is in a language other than English, please include an English translation.

**Experiment title:**Formation mechanism of  $\text{PbO}_2$  (plattnerite) by oxidative blackening of lead white in/on mural paintings by Cimabue (13th C.), Assisi Cathedral, Italy**Experiment number:**

HG-105

**Beamline:**

ID21

**Date of experiment:**

from: 01/07/2017 to: 04/07/2017

**Date of report:**

07/02/2020

**Shifts:**

9

**Local contact(s):**

Marine Cotte

*Received at ESRF:***Names and affiliations of applicants (\* indicates experimentalists):**

\* Letizia Monico, Department of Chemistry, Biology and Biotechnology, University of Perugia, Italy

\* Steven De Meyer, Department of Chemistry, Antwerp University, Belgium

\* Gert Nuyts, Department of Chemistry, Antwerp University, Belgium

## 1. INTRODUCTION

In mural paintings, the blackening of the pigment lead white [a mixture of cerussite ( $\text{PbCO}_3$ ) and hydrocerussite ( $2\text{PbCO}_3 \cdot \text{Pb}(\text{OH})_2$ )] has frequently been attributed to the formation of  $\beta\text{-PbO}_2$  (plattnerite, black). [1,2]

This phenomenon is clearly observable in a series of Cimabue's mural paintings (13th century) of *San Francesco Basilica* in Assisi (Italy).

During the 1997 earthquake, a portion of the vault of the Upper Basilica collapsed and a number of fragments of Cimabue's mural paintings showing blackening of brushstrokes that were originally white have been collected and conserved (Figure 1). [3]

The overall mechanism and the triggering factors of the oxidation process of lead white remain still poorly understood. [1-4]

With the main aim to clarify the reasons for the blackening of lead white leading to the formation of plattnerite, in this experiment we have employed a combination of  $\mu\text{-XANES}$  at Cl-K edge,  $\mu\text{-XRF}$  and  $\mu\text{-XRD}$  mapping for studying a series of mural painting samples originating from Assisi Cathedral and painted by Cimabue.

In order to assess how environmental factors and/or intrinsic properties of the paint (pH, light and chemicals, such as  $\text{Cl}^-$ ,  $\text{OCl}^-$ ,  $\text{HCO}_3^-$ ,  $\text{CO}_2$ ) may influence such process, the study of original paint fragments has been integrated with those of artificially aged model samples.

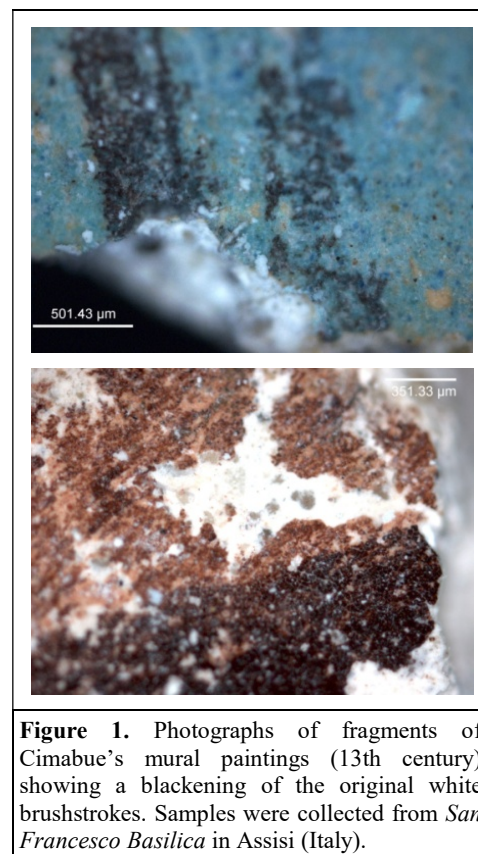


**Figure 1.** Photographs of fragments of Cimabue's mural paintings (13th century) showing a blackening of the original white brushstrokes. Samples were collected from *San Francesco Basilica* in Assisi (Italy).

## 2. EXPERIMENTAL

The list samples that we have analyzed at ID21-beamline is reported below:

*a) Artificially aged lead white-based model samples (10 in total)* before and after exposure to different aging conditions in presence and absence of Cl-species;

*b) Original paint micro-fragments from Cimabue's wall paintings (4 in total)* obtained from different blackened areas of the collapsed vault of *San Francesco Basilica* in Assisi.

By using the microtome available at the ID21-beamline, all samples were prepared as thin sections (average thickness of 5  $\mu\text{m}$ ); afterwards they were fixed on sulfur-free tape and were covered with an ultralene film.

Measurements were performed at the scanning X-ray microscope (SXM) end-station and at the scanning  $\mu$ -XRD/ $\mu$ -XRF end station. Investigations were carried out by means of a fixed exit double-crystal Si(111) monochromator at both the end-stations.

At the SXM-end station, the incident beam was focused with Kirkpatrick-Baez (KB) mirrors down to a diameter of *ca.*  $0.7 \times 0.4 \mu\text{m}^2$  (h $\times$ v). The energy calibration was performed using NaCl by setting the position of the peak maximum of their first order derivative spectrum at 2.8261 keV.

XRF signals were collected in the horizontal plane and at  $69^\circ$  with respect to the incident beam direction by means of a single energy-dispersive silicon drift detector (Xflash 5100, Bruker).

Single point  $\mu$ -XANES spectra were acquired in XRF mode by scanning the primary energy around the Cl K-edge absorption edge (2.79-2.89 keV; energy step: 0.25 eV).

$\mu$ -XRF mapping experiments were performed using a monochromatic primary beam of fixed energy around the Cl K-edge. Maps of the same region of interest were collected by employing either 80 or 100 ms/pixel at the two following energies: (i) 2.8216 keV (around the absorption edge), (ii) 2.8922 keV (in the post-edge absorption region). The software PyMCA was used to fit the XRF spectra and to separate the contribution of different elements, whilst ATHENA [5] was employed to perform the normalization of the XANES spectra.

At the  $\mu$ -XRD/ $\mu$ -XRF end station analysis were performed with an incident beam of 8.5 keV, that was focused down to a size of *ca.*  $2.0 \times 1.0 \mu\text{m}^2$  (h $\times$ v) by means of KB mirrors.  $\mu$ -XRD patterns were recorded using a taper FReLoN detector (2048 $\times$ 2048 pixels, pixel size 52  $\mu\text{m}$ ) and an exposure time of 10 s/pixel. XRD data has been processed by employing the software XRDUA. [6]

### 3. RESULTS

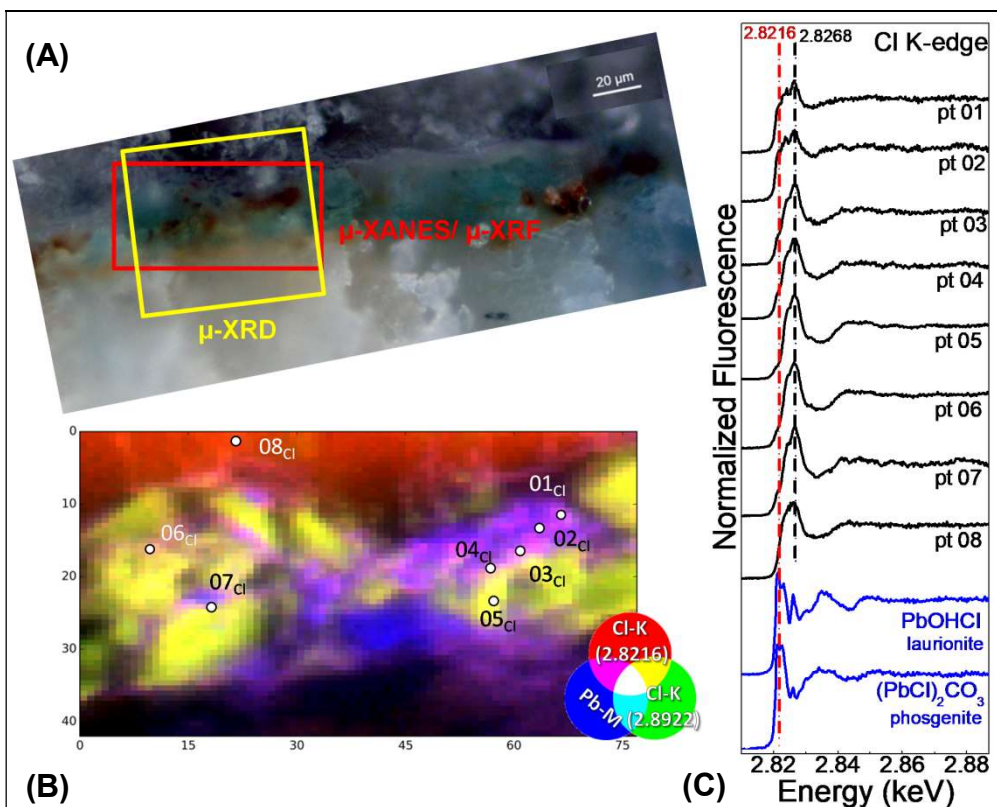


**Figure 1.** (A) Photomicrograph of a thin section obtained from a darkened fragment of a Cimabue's wall painting (*San Francesco Basilica*, Assisi, Italy), and (B) corresponding RGB composite SR  $\mu$ -XRF images of different Cl-species and Pb [step size (h×v):  $1 \times 0.7 \mu\text{m}^2$ , exp. time: 100 ms/pixel]. In (A), the rectangles show the area where map of (B) and  $\mu$ -XRD analysis (see Figure 2) were recorded. (C) Selection of Cl K-edge  $\mu$ -XANES spectra obtained from the points indicated in (B) compared to those of two (Pb,Cl)-based reference compounds.

Figure 1 illustrates the Cl-speciation results obtained from one of the analyzed thin sections, obtained from a darkened fragment of a Cimabue's wall painting.

Notably, the uppermost greenish layer shows the diffuse presence of Cl and Cu. The co-localized presence of Pb and Cl is observed in the brownish areas (Figure 1A,B).

The Cl-speciation maps, along with the corresponding Cl K-edge  $\mu$ -XANES spectra, reveal the presence of at least two different groups of Cl-compounds (Figure 1B,C). One group of spectra is characterized by the presence of a signal of variable intensity at *ca.* 2.8216 keV, that is assignable to (Pb,Cl)-based phases (pts 01-04). The other group of profiles (pts 05-07) shows instead mainly a spectral feature at about 2.8286 keV, which is likely characteristic of (Cu,Cl)-based compounds.

The  $\mu$ -XRD measurement (Figure 2) has further contributed to obtain information about the nature and stratigraphic distribution of the original/alteration crystalline compounds.

In the uppermost greenish-brownish layer, plattnerite ( $\beta$ -PbO<sub>2</sub>) and laurionite (PbOHCl) are likely present as a result of the alteration of the original lead white, [1-4] while paratacamite (a basic copper chloride) may be associated to the degradation of the blue/green pigment, azurite/malachite (copper carbonates). [7] In the same layer, quartz grains and whewellite [Ca(C<sub>2</sub>O<sub>4</sub>)·(H<sub>2</sub>O)] are also visible. The latter compound is also present together with gypsum in the yellowish layer underneath. Calcite is instead the main component of the ground layer.

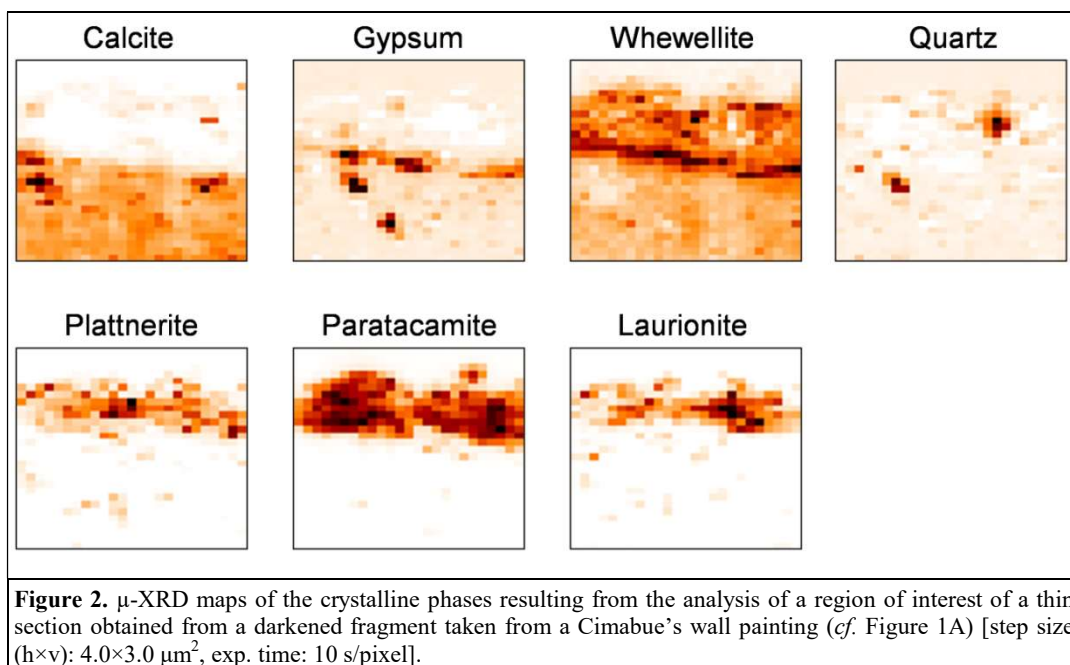


**Figure 2.**  $\mu$ -XRD maps of the crystalline phases resulting from the analysis of a region of interest of a thin section obtained from a darkened fragment taken from a Cimabue's wall painting (*cf.* Figure 1A) [step size (h×v):  $4.0 \times 3.0 \mu\text{m}^2$ , exp. time: 10 s/pixel].

Overall, the results obtained from original paint samples, along with those recorded from artificially lead white model samples (not reported), show the key-role of Cl-species in the blackening process of lead white. The data obtained from this experiment will be published soon.

#### REFERENCES:

- [1] S.M. Lussier, G.D. Smith, *Rev. Conserv.* **8** (2007), 41-53.
- [2] T. Rosado et al., *Color Res. Appl.* **41** (2016), 294-298.
- [3] M. Vagnini et al., *Vib. Spectrosc.* **98** (2018), 41-49.
- [4] E. Kotulanová et al., *J. Cultur. Herit.* **10** (2009) 367-378.
- [5] B. Ravel, M. J. Newville, *Journal of Synchrotron Radiation* **12** (2005), 537–541.
- [6] W. De Nolf et al., *Journal of applied crystallography* **47** (2014), 1107-1117.
- [7] S. Švarcová et al., *Analytical and bioanalytical chemistry* **395** (2009), 2037-2050.